Structural and Gasification Kinetic Studies on Co-pyrolysis Chars of Coal and Biomass

Lang Liu
Guizhou Institute of Technology
Jingsong Zeng
Chongqing University
Qingrui Jiao (406138767@qq.com)
Chongqing University
Shan Ren
Chongqing University
Jian Yang
Chongqing University
Xiangdong Su
Guizhou Institute of Technology
Yan Cao
Guangzhou Institute of Energy Conversion
Anjiang Tang
Guizhou Institute of Technology

Research Article

Keywords: char gasification, kinetic fitting, char characteristics, gasification reactivity

Posted Date: May 21st, 2021

DOI: https://doi.org/10.21203/rs.3.rs-524028/v1

Version of Record: A version of this preprint was published at Energy Advances on January 1st, 2022. See the published version at https://doi.org/10.1039/D1YA00071C.

Abstract

In the present study, the CO_2 gasification behaviours of the co-pyrolysis chars with coal and biomass as feedstock were investigated using isothermal thermogravimetric analysis (TGA) at 950–1150 °C. The TGA results demonstrated that the char gasification reactivity was improved at higher biomass composition. In addition, the char characteristics results evaluation revealed that biomass promoted the development of a porous structure and inhibited the formation of graphite-like carbon during the co-pyrolysis of coal and biomass. Moreover, an extended random pore model (eRPM) was proposed to define the char gasification kinetics of coal and biomass. It was found that the activation energies of chars decreased with increasing biomass composition. Lastly, the relationship between the gasification reactivity and char characteristics was evaluated.

Highlights

- Catalytic mechanism of biomass addition on char gasification was studied
- K in biomass affects both of the porous and crystalline characteristics of char.
- An eRPM was proposed to define the co-pyrolysis char gasification kinetics.
- Char gasification reactivities correlate well with char characteristics.

1. Introduction

Coal is widely considered as a steady fossil fuel that can be directly burned or transformed into other energy forms. Nevertheless, the utilisation of coal has exacerbated various environmental problems, such as the emissions of SO_2, NO_x, and greenhouse gases (GHG). Compared to combustion, coal gasification to syngas is an effective way to produce power, heating, and syngas fuel on a large-scale, enabling simultaneous capture and storage of CO_2 [1].

Various catalysts have been proposed to enhance coal gasification processes [2, 3]. Numerous studies have shown that alkali, alkaline earth, and transition metals, such as K, Na, Ca, and Fe, can significantly improve the activity of char gasification [4–6]. Notably, the alkali metals exhibit the best catalytic activity a result of the formation and diffusion of the liquid-solid interface between the alkali and the carbon surface [7, 8]. However, a significant amount of alkali metals is volatilised to the gas phase during the gasification process at high temperatures. In addition, the strong interactions between alkali metals and minerals in coal can lead to catalyst deactivation as well as difficult recovery and regeneration [9–11].

Thus, the development of inexpensive and abundant catalysts is essential. It is widely known that biomass is rich in alkali metals, which can be used as catalysts to enhance the char gasification efficiency[12, 13]. F. Pinto et al. [14] reported that the biomass composition should not exceed 10% due to the high surface tension of co-gasification of edible oil waste and coal. Moreover, depending on the fuel specifications and calorific value, Nasrin et al.[15] suggested that the blending ratio for biomass in mixtures with coal should be in the range of 5–10%. On the other hand, Meanwhile, Li et al.[16] proposed a blending ratio of 0–33% for pine sawdust blended with coal.

In a typical gasifier, such as the fixed bed dry bottom (FBDB) gasifier, the feedstock gasification is processed under high temperature and pressure. Furthermore, the gasifier is subjected to different reaction zones, i.e., drying, pyrolysis, and gasification[17]. Pyrolysis is the pre-step to gasification and involves cracking of the organic matter in coal, volatilisation of low molecular weight pyrolysis products, polycondensation of cracking residues, decomposition and combination of volatile products during emission, and further decomposition and repolycondensation of the polycondensation products [18, 19]. It is noteworthy that all of these processes affect the characteristics of char fed into the gasification zone.

Char gasification is generally considered as the rate-limiting step of the entire process [20]. Furthermore, the characteristics of char, such as the chemical and structural properties as well as ash composition, influence the char gasification reactivity [21]. Ahmadet al. [22] and Everson et al.[23] previously determined that gasification reactivity increased with a decrease in aromaticity of various raw materials, including lignocellulose biomass and coal. Huo et al.[24] reported that the reactivity index ($R_{0.5}$) increased with an increase in the interlayer spacing (d_{002}) and a decrease in the crystallisation height (L_c). Moreover, Zhang et al. [25] quantitatively analysed the degree of interaction between biomass and coal during gasification and pyrolysis using the synergy factor. Nevertheless, the relationship between the chemical and structural characteristics of char in relation to the co-gasification reactivity has not been sufficiently investigated.

Notably, co-gasification of coal and biomass first involves co-pyrolysis. Furthermore, it has been shown that addition of biomass has an important influence on the co-pyrolysis process and affects the characteristics of the initial chars. The minerals in biomass also have a significant impact on gasification. Specifically, the interactions between minerals or between char and minerals during char gasification exhibit synergistic effects on the process [26].

Hence, in this study, coal and biomass mixtures with different ratios (0, 5%, 10%, 15%, 20%) were co-pyrolyzed. Subsequently, the activity of the gasification reaction of co-pyrolysis chars was evaluated using a thermogravimetric analyser (TGA). The investigation of the gasification reaction kinetics was conducted by defining the random pore model (RPM) as well as the extended RPM. In addition, the characteristics of the co-pyrolysis char were quantitatively characterised by the Brunauer–Emmett–Teller (BET), Scanning Electron Microscopy (SEM), X-ray powder diffraction (XRD), and Raman spectroscopy analyses. Finally, the relationship between the selected characteristics of the co-pyrolysis chars, such as the porous structure and crystallite properties, and the co-gasification kinetic parameters (i.e., activation energy and pre-exponential factor) was analysed. The current study enhances the current knowledge on co-gasification of coal and biomass. The results obtained herein could be used for the design of highly efficient gasifiers.

2. Materials And Methods

2.1 Materials

In this work, a typical coal in Southwest China was selected as the coal sample, while wheat straw was chosen as the biomass sample. The proximate and ultimate analyses of the raw samples are summarised in Table 1. The raw samples were milled and sieved into particles sized between 74 and 100 μm. The coal

powders were subsequently blended with the biomass in a mixer for 10 min. The blending proportions were as follows: biomass 0%/coal 100%, biomass 5%/coal 95%, biomass 10%/coal 90%, biomass 15%/coal 85%, biomass 20%/coal 80%.

Table 1
Proximate and ultimate analysis of the raw samples

Sample	Proximate analysis (wt%, db)				Ultimate analysis (wt%, daf)					Calorific value (J/g)
	Fixed carbon	Volatiles	Ash	Moisture	C	H	N	O[b]	S	
Coal	74.5	15.63	9.47	0.4	81.49	4.26	1.22	12.45	0.56	32490
WS	11.42	73.49	8.54	6.55	41.02	3.83	1.724	53.13	0.28	16201.1

db, dry basis; and daf, dry and ash-free, [b] oxygen content by difference.

2.2 Preparation and characterisation of chars

The co-pyrolysis chars were prepared at 1150°C under a N_2 atmosphere in a horizontal tubular furnace. 800 mg of the char mixture was evenly spread on crucible boats, and then heated to 1150°C under a N_2 atmosphere at heating rate of 20°C/min. The feedstock was kept at the set temperature for 30 min.

The chemical characteristics of the chars were analysed using a wide-angle XRD analyser (Ultima IV), DXR Raman spectrometer (Thermo Fisher Scientific). The structural features were charactered by a N_2 adsorption-desorption isotherms apparatus (ASAP 2020) and a Nova Nano SEM 450 microscope (FEI Company).

2.3 Preparation and characterisation of char ash

The ash samples of the co-pyrolysis char were prepared according to the standards ASTM E1755-01. About 1g co-pyrolysis char samples was laid flat in a corundum crucible and placed in a muffle furnace. Firstly, heating the samples to 250 ^{o}C and kept for 30 min, and then rising the temperature to 575 ^{o}C within 30 min and held for 3 h, while the heating rate was 10 ^{o}C/min. This ash preparation under such a procedure is to avoid the possible phase change and volatilization of minerals because of flame burning. The ash composition was evaluated by X-ray fluorescence (XRF) spectroscopy (PANalytical Axios and the mineral phases in ash samples were analysed using the wide-angle XRD analyser (Ultima IV).

2.3 Gasification experiment

Water and CO_2 are two regular gasification agents, but water is recently limited to reach in the energy development sector, and CO_2 can be obtained from the iG-CLC system itself, thus CO_2 was selected as the gasification agents in this study. The CO_2 gasification experiment was conducted in a Netzsch STA 449F3 thermogravimetric analyser under a CO_2 atmosphere in the temperature range of 950–1150°C. In the gasification experiment, 5 ± 0.1 mg samples were thinly dispersed on a crucible plate, heated to 950–1150°C at a heating rate of 20°C/min under a 100 mL/min N_2 stream, and then held for 30 min to fully pyrolyze the

samples. Subsequently, the N_2 stream was switched to a 100 mL/min CO_2 stream to initiate the gasification for 90 min.

2.4 TGA data Analysis

The CO_2 gasification process of char is a typical gas-solid heterogeneous reaction. In the study of gasification characteristics and kinetic behaviour, the data of gasification weightlessness need to be converted to conversion rate. The gasification conversion (X) of the sample during gasification was calculated according to Eq. 1:

$$X=\frac{m_o-m_t}{m_o-m_{ash}} \quad (1)$$

where, m_o is the initial char mass, m_t indicated the char mass at instantaneous time t, and m_{ash} denotes the ash mass.

The CO_2 gasification rates (R) were determined using Eq. 2:

$$R=\frac{dX}{dt} \quad (2)$$

3. Results And Discussion

3.1 Char gasification activity tests

The TGA profiles of the gasification of co-pyrolysis chars in CO_2 under isothermal conditions (950–1150°C) are illustrated in Fig. 2(a–c). As expected, the biomass exerted a positive effect on the CO_2 char gasification. Specifically, the carbon conversion increased with increasing biomass composition at a given gasification temperature. This is mainly due to the rich alkali metals in biomass, as shown in Table 2, which play a catalytic role in the char gasification. This result was consistent with the outcomes of the previous studies, which concluded that some types of biomass can be applied as cheap and abundant catalysts to promote gasification [27].

Table 2
Chemical composition of the ash

Sample	Ash chemical composition (wt.%)									
	SiO_2	Al_2O_3	SO_3	CaO	Fe_2O_3	K_2O	TiO_2	MgO	Na_2O	others
0% bio	58.76	21.68	4.79	4.83	4.21	1.45	1.68	0.93	0.85	0.82
5% bio	57.78	20.33	5.48	4.87	4.05	2.61	1.62	1.24	1.01	1.01
10% bio	57.03	19.06	5.97	5.01	3.85	3.65	1.53	1.5	1.17	1.23
15% bio	56.55	17.61	6.33	5.13	3.71	4.66	1.46	1.78	1.31	1.46
20% bio	55.71	16.16	7.2	5.24	3.49	5.67	1.35	2.06	1.44	1.68

3.2 Catalytic mechanism analysis

As known, the char gasification mainly involves the adsorption and desorption process of C-O complex[28]: the active site C_f on the char reacts with CO_2 to form CO and the intermediate C(O) containing O on the surface, and then the CO separates from the intermediate to produce the active site of char. Therefore, the gasification reactivity of char is directly related to the active carbon sites.

$$C_f + CO_2 \leftrightarrow C(O) + CO$$

$$C(O) \rightarrow CO$$

The catalytic mechanism of the char gasification mainly includes oxygen transfer theory, electrochemical theory and intermediate theory. According to the theory of oxygen transfer[8], the catalyst acts as the intermediate of oxygen storage and transfer in carbon gasification. According to the electrochemical theory [29], the catalyst transfers the charge of carbon skeleton on coal surface through partial bonding with C atom, changes the electron cloud distribution of carbon skeleton on char surface, weakens the binding strength of C-C bond, enhances the binding force of C-O bond, and makes the surface of char have more reactive sites. According to the intermediate theory [30], the catalyst forms an electron donor receptor (EDA) complex with aromatic carbon in carbon. EDA has strong catalytic activity and can catalyse the reactions of C-H_2, C-H_2O and C-CO_2. However, due to the complexity of biomass components and carbon structure, so far, there is lacking of understanding of the catalytic mechanism of the biomass addition on the char gasification.

The characteristics of carbon structure, such as molecular structure, crystal structure, active sites concentration and surface area, have a direct impact on the active carbon sites.

In order to reveal the mechanism of biomass addition on char gasification, the mineral components in the co-pyrolysis char ash were analyzed, as summarised in Table 2. The obtained results showed that SiO_2 and Al_2O_3 were the key components in the ash samples. The two oxides accounted for > 70% of the total composition. It was also found that the proportions of K_2O significantly increased with the increasing of

biomass proportion. In contrast, the proportions of CaO, MgO, and Na_2O only increased slightly, while the amounts of SiO_2, Al_2O_3, Fe_2O_3, and TiO_2 decreased with increasing proportion of biomass. These outcomes suggested that the selected biomass was rich in potassium, which could act as a catalyst in the gasification of co-pyrolysis char.

Several researchers previously reported that the presence of potassium in biomass was conducive to increasing the amount of active sites on the carbon surface during gasification [31, 32]. Thus, the morphologies of the co-pyrolysis chars were charactered by the SEM firstly, as shown in Fig. 3. It can be found that the surface of the coal char was compact without obvious pore structure, and only a few small particles adhere to the surface. After mixing 5% WS into co-pyrolysis process, the surface becomes rough, and the number of small particles on the surface increases obviously, and a few small pore structures can be found. With increasing WS proportion to 10%, the original small grooves on the surface of char begin to expand and form a large number of lamellar structures, and the pore structure has developed significantly regardless of size or depth, and most of the small particles adhere to the lamellar structures. When WS proportion increases to 15%, the lamellar structures deepen, the pore structure continues to increase, and the small particles attached to the lamellar structures decrease gradually. While, the gully structure disappeared in the co-pyrolysis char with 20% WS, which developed to larger pore structure, and there were a few pore structures with smaller pore size around the macropore. During the co-pyrolysis of biomass and coal, alkali metals begin to adsorb in the initial pores of char, and then gradually diffuse into the inner carbon matrix. Alkali metals are embedded in the graphite layer of coke carbon matrix to form alkali metal graphite intercalation compounds, such as KC6 and KC60 [33]. In this process, the internal stress of carbon matrix increases, resulting in the volume expansion of char. In addition, the reaction of alkali metals with other minerals in char will also cause the volume expansion of minerals, and then change the structure of char. In the gasification process, the large number of layered structures make the char structure loose, which makes it easier to react with CO_2.

The XRF of the ash and the SEM results of the char together illustrated that the presence of alkali metals (especially potassium) in biomass plays an important role in the development of the porous structure [34, 35], and led to an increase the amount of active sites on the carbon surface per unit weight [31, 32]. The reaction between alkali metals and other minerals in char will resulted in the expansion of mineral volume, which is conducive to the development of pore structure [36]. Moreover, alkali metals in the biomass will adsorbed on the surface of the char first and then gradually diffused into the internal carbon structure and embedded in the graphite layer to form alkali metal-graphite intercalation compounds which also will resulted in the expansion of pore structure of char[33].

The results of previous studies also demonstrated that alkali metals significantly affected the carbon crystallite characteristics, including the crystallisation height (L_c), microcrystalline size (L_a), and crystal layer spacing (d_{002})[21, 34]. The results of the XRD analysis the prepared chars are presented in Fig. 4. The minor peaks in the patterns were caused by the presence of inorganic minerals in coal and biomass, while the sharp peaks at approximately 27° was attributed to the existence of SiO_2. Furthermore, the (002) band at ~ 25° and the (100) band in the vicinity of graphite at ~ 43° [37] corresponded to graphite-like structures (i.e., crystalline carbon). The appearance of γ peaks at approximately 20° suggested the existence of aliphatic

side chains attached at the periphery of the carbon crystallites [38]. The obtained outcomes implied that the structures of the carbon crystallites were between graphite and the amorphous state.

Figure 5 illustrates the XRD patterns after smoothing and processing by Peakfit 4.2. It was found that the intensity of the (002) and (100) bands decreased with an increase in the biomass proportion, which indicated that biomass doping could inhibit the graphitisation of char during pyrolysis. The results also demonstrated that the intensity of the *γ* peak increased with an increase in the biomass proportion. It was speculated that this was caused by the inhibition of the breaking of the side chains in the aliphatic moieties by the catalyst components in the biomass during pyrolysis. It was also hypothesised that there were more aliphatic chains in raw biomass than in raw coal.

The calculated L_a, L_c, and d_{002} values are shown in Fig. 6. As it can be seen, the values of L_a and L_c decreased with an increase of the biomass proportion. In contrast, the values of d_{002} exhibited a reverse trend. These observations indicated that the order of aromatic moieties in the sample was more irregular in space, this is due to as the increasing of biomass addition, the content of alkali metals in the co-pyrolysis char increased, especially potassium, which means more alkali metals atoms penetrate into the carbon structure and occurs intercalation reaction, which affects the carbon microcrystalline structure of char disintegrate and makes the carbon structure become looser. in a word, the addition of biomass makes the microcrystalline structure of carbon develop to reverse graphitisation during co-pyrolysis. The ash XRD patterns of the co-pyrolysis char was shown in Fig. 7, the alkali metals in char samples mainly exist as $KAlSiO_4$ and $NaAlSi_3O_8$, when the biomass content increases, the peak of $KAlSiO_4$ becomes sharper, which indicates that K in biomass reacts with other ash contents to form $KAlSiO_4$.

To further verify the XRD results of the chars, we conducted Raman spectroscopy analysis to evaluate the chemical features of highly disordered carbon in the co-pyrolysis chars. We averaged multiple Raman spectra of each sample to account for the heterogeneity of the char particles. The Raman spectra obtained in the range from 800 to 2000 cm^{-1} are illustrated in Fig. 8.

The spectra were deconvoluted into four Lorentzian bands (designated as the G, D1, D2, and D4 bands) and one Gaussian band (labelled as the D3 band). The D1 band at ~ 1350 cm^{-1} was attributed to the vibration between the aromatic rings and aromatic moieties with no less than six rings. It belonged to the A_{1g} vibration of the amorphous hexagonal irregular lattice structure, and represented disorder in the carbon structure [39]. The D2 band was detected at the shoulder band of the G band, which corresponded to the vibrational mode of the disordered graphite lattice. It was attributed to the E_{2g} mode of the symmetric graphite lattice [40]. On the other hand, the D3 band observed at ~ 1500 cm^{-1} was ascribed to the amorphous sp^2-bonded forms of carbon [41, 42]. In addition, the D4 band at ~ 1250 cm^{-1} was attributed to amorphous mixing of the sp^2–sp^3-bonded forms of carbon. Lastly, the G band was the graphitic band. Subsequently, the band area ratios $(I_{D1} + I_{D3} + I_{D4})/I_G$ and I_G/I_{all} were calculated to indicate the reacting sites and the extent of graphitisation in the co-pyrolysis chars. The variation of the band area ratios $(I_{D1} + I_{D3} + I_{D4})/I_G$ and I_G/I_{all} with the biomass proportion is shown in Fig. 9. The results implied that $(I_{D1} + I_{D3} + I_{D4})/I_G$ increased with increasing biomass proportion, while I_G/I_{all} exhibited a reverse trend. This suggested that the

graphitic microcrystallite size decreased. Importantly, the Raman spectroscopy analysis was consistent with the XRD evaluation.

3.2 Kinetic analysis

The char-CO_2 gasification mainly involves the adsorption and desorption process of C-O complex: CO_2 in the atmosphere diffuses to the surface of particles and adsorbs on these surfaces, and then reacts with carbon; the reaction product desorbs and diffuses from the surface to the outside of the particles, which means all of the chemical reaction rate, internal diffusion rate and external diffusion rate may become the limiting-step in the char gasification. Therefore, it is necessary to analyse the limiting-step before studying the char gasification kinetics. Figure 10 shows that the relationship between ln(R) and 1/T at different gasification conversion (X) presents a good linear relationship, with $R^2 \geq 0.95$, which indicated that the investigated gasification reactions were Regime I and under chemical reaction control.

Random pore model (RPM) has been proposed as the optimal model to define the char gasification kinetics under chemical reaction control, which can address the char structure evolution during gasification. The gasification rate and carbon conversion curves were first defined by RPM (Fig. 11 (a–c)). As it can be seen, the gasification rate initially increased and then decreased with carbon conversion. Moreover, the maximum gasification rate was noted at a carbon conversion of 0.25–0.4. However, RPM was not a suitable model for the prediction of char gasification behaviours. This is due to the synergistic effects of the interactions between carbon and minerals as well as between minerals themselves during char gasification.

Thus, considering the assumptions of RPM and basing on the specific characteristics of the obtained experimental data, an extended RPM model is proposed in this work. Meanwhile the following assumptions are made in this model:

1. The char particles are porous, and the pores are cylindrical holes with uneven diameters, and the CO_2 gasification predominantly occurs on the inner surface of the char particles;
2. The variation in the reaction area is a result of the interaction between the pore structures and the consumption of carbon active sites;
3. In the initial stage of gasification, CO_2 rapidly reacts with the amorphous carbon structures, leading to a gradual decrease in the amorphous carbon content, the subsequent main reaction between CO_2 and the aromatic carbon structure is very slow;
4. The interactions between carbon and minerals as well as between minerals themselves affect the pore structures of chars, the interactions between carbon and minerals also affect the carbon crystallite characteristics, and these interactions is related to gasification conversion.

Based on the conducted calculations, it was determined that the influence of the interactions between carbon and minerals as well as between minerals themselves on the entire gasification process can be expressed by the following equation (Eq. 3):

$$G(x) = e^{x}(1-x)^{\alpha} \qquad (3)$$

An extend random pore model (eRPM) will be obtained by putting the Eq. 3 into RPM, as shown in Eq. 4.

$$\frac{dx}{dt} = ke^{x}(1-x)^{\beta}\sqrt{1-\psi\ln(1-x)} \qquad (4)$$

where, α indicates a dimensionless dimension related to the mineral composition and gasification temperature, ψ is the porous structural parameter.

Thus, a semi-empirical formula ($G(x)$) was introduced to the original RPM, which was named eRPM (Eq. 3). The corresponding fitting results are shown in Fig. 12 (a–c). Notably, significantly better fitting results were obtained employing eRPM than RPM. In addition, the experimental data was consistent with the theoretical data calculated by eRPM. Importantly, as shown in Table 3, most of the R^2 values were high ($R^2 \geq 0.99$). It was also found that the k values increased with increasing biomass composition at a given temperature, which confirmed the catalytic effect of biomass. The calculated α values ranged between 0.69 and 1.70. Furthermore, the ψ values for gasification of the prepared chars were in the range of 4.5–26.16. The above calculations confirmed that eRPM proposed in the present study could accurately describe the kinetic behaviour of char gasification. Moreover, it was demonstrated that the synergistic effects of the interactions between chars and minerals as well as between minerals themselves on the gasification reaction were valid.

Table 3
Kinetic parameters and R^2 values calculated by eRPM.

Temperature	Parameter	Sample				
		0% bio	5% bio	10% bio	15% bio	20% bio
950 °C	R^2	0.97	0.99	0.99	0.99	0.99
	k	0.0024	0.0039	0.0063	0.0087	0.011
	α	1.21	1.23	1.28	1.67	1.70
	ψ	24.14	26.16	14.43	17.33	22.01
1050 °C	R^2	0.99	0.99	0.99	0.99	0.99
	k	0.026	0.028	0.033	0.045	0.056
	α	0.92	0.95	1.04	1.22	1.34
	ψ	15.43	14.73	14.19	11.17	10.02
1150 °C	R^2	0.99	0.99	0.99	0.99	0.99
	k	0.094	0.11	0.12	0.14	0.15
	α	0.96	0.96	1.00	0.86	0.69
	ψ	8.09	6.75	5.97	5.13	4.51

The above calculations confirmed that eRPM proposed in the present study could accurately describe the kinetic behaviour of co-gasification. Moreover, it was demonstrated that the synergistic effects of the interactions between chars and minerals as well as between minerals themselves on the gasification reaction were valid. Hence, *G(x)* in Eq. 3 could be used to predict the synergistic influence of the above interactions on the entire co-gasification process. The relationship between these effects and the gasification conversion is demonstrated in Fig. 13 (a–c). Furthermore, Fig. 13(a–c) shows that the catalytic effect of minerals on co-gasification gradually decreased during gasification. This was caused by the gradual consumption of the carbon matrix as well as by the strengthening of the interactions between minerals, which resulted in the deactivation of the catalyst [9]. The data shown in the above figures also indicated that the catalytic effects of the catalyst component on co-gasification decreased with increasing biomass proportion when the temperature was below 1050°C. We speculated that this was caused by the inhibition of the carbon lattice growth by the catalyst component in biomass and by the enhancement of the production of volatile matter, which in turn resulted in an increased amount of reactive sites in co-pyrolysis char. In addition, as shown by the XRD and Raman spectroscopy analyses, the amount of reactive sites increased with an increase in the biomass proportion [43]. In contrast, the effect of the catalyst on the amount of reactive sites was smaller. Figure 13c demonstrates that when the temperature was raised to 1150°C and the biomass increased to 15%, the interaction between the catalyst and char, particularly the graphite-like carbon matrix, was enhanced, and the catalytic effect of the catalyst was improved.

The Arrhenius law was applied to determine the activation energy (E_a) and pre-exponential factor (k_0) values according to the following equation (Eq. 5):

$$k = k_0 \exp(-E_a / RT) \qquad (5)$$

where, T is the absolute isothermal gasification temperature and R indicates the universal gas constant. The k values obtained from eRPM were used to calculate the values of E_a and k_0. The Arrhenius plots ($\ln k$ vs. 1/T) acquired by linearising plots obtained by Eq. 5 are shown in Fig. 14. In addition, the calculated E_a and k_0 values are summarised in Table 4. It was found that the E_a values of chars decreased from 266.5 to 190.8 kJ/mol with an increase in the biomass composition from 0 to 20%. The decrease of the E_a values further confirmed the catalytic activity of the biomass.

Table 4
The E_a, k_0, and R^2 values for the char gasification reaction based on eRPM.

Sample	E_a (kJ/mol)	lnk_0	R^2
0% bio	266.5	20.30	0.97
5% bio	240.2	18.14	0.99
10% bio	216.4	16.23	0.99
15% bio	198.9	14.88	0.99
20% bio	190.8	14.32	0.98

The char gasification is almost simultaneous with the reduction reaction of oxygen carriers, while the carbon crystallite and structural characteristics of the chars exhibit direct effects on the gasification reactivity. Studying the relationship between gasification reactivity and char microstructure can help to further understand the char gasification behaviours in the iG-CLC process. The diagram of the relationships between the char parameters (i.e., S_{BET}, L_a, L_c, $(I_{D1} + I_{D3} + I_{D4})/I_G$, and I_G/I_{all}) and the activation energies is illustrated in Fig. 15. The results indicated that most of the parameters (i.e., S_{BET}, L_c, $(I_{D1} + I_{D3} + I_{D4})/I_G$ and I_G/I_{all}) displayed linear correlations with the activation energies ($R^2 \geq 0.95$). On the other hand, 2nd order polynomial correlation was noted between the L_a parameter and the activation energies. Based on the values of R^2, the crystallite characteristics, and therefore aromaticity, had a significant impact on the activation energies[44]. These observations indicated that the crystallite characteristics governed the char gasification rates during experiments conducted in a thermogravimetric analyser. Additionally, the structural characteristics of char also had an important effect on the reactivity of gasification of co-pyrolysis char. Overall, we determined that the reactivity of gasification of co-pyrolysis char composed of coal and biomass could be predicted based on characteristic char parameters, such as S_{BET}, L_a, L_c, $(I_{D1} + I_{D3} + I_{D4})/I_G$, and I_G/I_{all}.

4. Conclusions

The kinetics and structure of co-pyrolysis char using coal and biomass mixture as feedstocks were studied through isothermal thermogravimetric analysis method. The results indicated that biomass addition is beneficial to development of pore structure and reverse graphitization of carbon structure, which is in a result of the synergistic effects of the interactions between chars and minerals (especially potassium), as well as between different minerals, and this synergy exists throughout the gasification process. The investigated gasification reactions were demonstrated as the Regime I and under chemical reaction control, and an eRMP was proposed to define the synergistic effects of the interactions between chars and minerals as well as between different minerals on char gasification, which was found to accurately determine the kinetics of co-pyrolysis char gasification. Meanwhile, the relationship between char characteristics, such as the S_{BET}, L_a, L_c and $(I_{D1} + I_{D3} + I_{D4})/I_G$, and the kinetic parameters (E_a) was investigated, the results showed a

statistically significant correlation. In addition, the activation energies decreased with increasing biomass proportion.

Declarations

Declaration of interests

The authors declared that they have no conflicts of interest to this work.We declare that we do not have any commercial or associative interest that represents a conflict of interest in connection with the work submitted.

Author contributions

Lang Liu and Jian Yang contributed to the conception and design of this study; Jingsong Zeng and Qingrui Jiao performed the experiment and data analysis; Shan Ren, Xiangdong Su, Yan Cao and Anjiang Tang helped perform the analysis with constructive discussions.

Data availability statement

The datasets generated during and/or analysed during the current study are available from the corresponding author on reasonable request.

Acknowledgements

The work is financially supported by the Youth Science and Technology Talents Growth Project of Guizhou Provincial Education Department ([2017]220), the Science and Technology Planning Project of Guizhou province ([2018]1066), Young Teachers Training Project of Guizhou Institute of Technology ([2017]5789-05), and National Natural Science Foundation of China (No. 51874058).

References

1. Giuffrida A, Bonalumi D, Lozza G (2013) Amine-based post-combustion CO_2 capture in air-blown IGCC systems with cold and hot gas clean-up. Appl Energy 110:44–54
2. Daunt N, Ross M, Couzens G, Cutbush K, Green J, Kennedy D, Keller J (2014) K_2O_3 catalyzed CO_2 gasification of ash-free coal. Interactions of the catalyst with carbon in N_2 and CO_2 atmosphere. Fuel 117:1181–1189
3. Ohtsuka Y, Asami K (1997) Highly active catalysts from inexpensive raw materials for coal gasification. Catal Today 39:111–125
4. Xie Y, Zhang C, Wang D, Lu J, Zhang R (2019) Catalytic performance of the Bi_2O_3-Fe_2O_3 system in soot combustion[J]. New J Chem 43:15368–15374
5. Yeboah YD, Xu Y, Sheth A, Godavarty A, Agrawal PK (2003) Catalytic gasification of coal using eutectic salts: identification of eutectics. Carbon 41:203–214

6. Zhang Y, Zhao J, Wei X, Li T, Xu M (2019) Effects of alkali metals on the formation of PM and adsorption of floating beads during Zhundong coal combustion[J]. Energy Fuels 33:5422–5429
7. Zhu H, Wang X, Wang F, Yu G (2018) In Situ Study on K_2CO_3-Catalyzed CO_2 Gasification of Coal Char: Interactions and Char Structure Evolution. Energy Fuels 32:1320–1327
8. Mckee DW, Spiro CL, Kosky PG, Lamby EJ (1983) Catalysis of coal char gasification by alkali metal salts. Fuel 62:217–220
9. Kühn L, Plogmann H (1983) Reaction of catalysts with mineral matter during coal gasification. Fuel 62:205–208
10. Zhao Y, Zhang W, Wang P, Liu P, Zeng G, Sun S, Zhang S (2018) Kinetic characteristics of in-situ char-steam gasification following pyrolysis of a demineralized coal. Int J Hydrogen Energy 43:10991–11001
11. Chen X, Liu L, Zhang L, Zhao Y, Qiu P (2019) Gasification reactivity of co-pyrolysis char from coal blended with corn stalks. Bioresour Technol 279:243–251
12. Jeong HJ, Sang SP, Hwang J (2014) Co-gasification of coal-biomass blended char with CO2 at temperatures of 900–1100 C. Fuel 116:465–470
13. Yan L, Cao Y, Li X, He B (2018) Characterization of a dual fluidized bed gasifier with blended biomass/coal as feedstock. Biores Technol 254:97–106
14. Pinto F, Lopes H, Rui NA, Gulyurtlu I, Cabrita I (2007) Effect of catalysts in the quality of syngas and by-products obtained by co-gasification of coal and wastes. 1. Tars and nitrogen compounds abatement. Fuel 86:2052–2063
15. Nasrin AB, Ma AN, Chow MC, Hamdan H, Choo YM (2006) Blending of palm biomass and coal: An alternative fuel for power generation in Malaysia. Oil Palm Industry Economic Journal 6:31–36
16. Li K, Rong Z, Bi J (2010) Experimental study on syngas production by co-gasification of coal and biomass in a fluidized bed. J International Journal of Hydrogen Energy 35:2722–2726
17. B.J. R., W. F.B., Identification of the reaction zones occurring in a commercial-scale Sasol-Lurgi FBDB gasifier, Fuel 87 (2008) 1814–1823
18. SOLOMON RP (1993) FLETCHER, H. T., PUGMIRE, J. R., Progress in coal pyrolysis. Fuel 72:587–597
19. IBARRA VJ, BONET MOLINER (1994) J. A., FT-i.r. investigation on char formation during the early stages of coal pyrolysis. Fuel 73:918–924
20. Liu L, Cao Y, Liu Q (2015) Kinetics studies and structure characteristics of coal char under pressurized CO_2 gasification conditions[J]. Fuel 146:103–110
21. Mafu LD, Neomagus H, Everson RC, Okolo GN, Strydom CA, Bunt JR (2018) The carbon dioxide gasification characteristics of biomass char samples and their effect on coal gasification reactivity during co-gasification. Bioresour Technol 258:70–78
22. Ahmad A (2016) Atikah, Khasri, Azduwin, Kasim, Farizul, Hafiz, Inayat, Abrar, Assessing the gasification performance of biomass: A review on biomass gasification process conditions, optimization and economic evaluation. Renewable Sustainable Energy Reviews 53:1333–1347
23. Everson RC, Okolo GN, Neomagus HWJP, Santos JMD (2013) X-ray diffraction parameters and reaction rate modeling for gasification and combustion of chars derived from inertinite-rich coals. Fuel 109:148–

156
24. Huo W, Zhou Z, Chen X, Dai Z, Yu G (2014) Study on CO2 gasification reactivity and physical characteristics of biomass, petroleum coke and coal chars. Bioresour Technol 159:143–149
25. Zhang Y, Zheng Y, Yang M, Song Y (2016) Effect of fuel origin on synergy during co-gasification of biomass and coal in CO_2. Bioresour Technol 200:789–794
26. Ding L, Zhang Y, Wang Z, Huang J, Fang Y (2014) Interaction and its induced inhibiting or synergistic effects during co-gasification of coal char and biomass char. Bioresour Technol 173:11–20
27. Wang X, Yao K, Huang X, Chen X, Yu G (2019) Effect of CaO and biomass ash on catalytic hydrogasification behavior of coal char. Fuel 249:103–111
28. Mentser M, Ergun S, A Study of the Carbon Dioxide-Carbon Reaction by Oxygen Exchange, Technical Report Archive & Image Library (1973)
29. Jalan BP, Rao YK (1978) A study of the rates of catalyzed Boudouard reaction. Carbon 16:175–184
30. Wen (1980) Mechanisms of Alkali Metal Catalysis in the Gasification of Coal, Char, or Graphite. Catalysis Reviews 22:399–401
31. Standish N, Tanjung AFA (1988) Gasification of single wood charcoal particles in CO_2. Fuel 67:666–672
32. JA M, Kapteijn F (1995) Towards a unified theory of reaction of carbon with oxygen-containing molecules. Carbon 33:1155–1165
33. Wang G, Ren S, Zhang J, Ning X, Liang W, Zhang N, Wang C (2020) Influence mechanism of alkali metals on CO 2 gasification properties of metallurgical coke. Chem Eng J 387:124093
34. Gong X, Guo Z, Wang Z, Gong X, Guo Z, Wang Z (2009) Variation of Char Structure during Anthracite Pyrolysis Catalyzed by Fe_2O_3 and Its Influence on Char Combustion Reactivity[J]. Energy Fuels 23:4547–4552
35. Mckee DW (1983) Mechanisms of the alkali metal catalysed gasification of carbon[J]. Fuel 62:170–175
36. Reyes S, Jensen KF (1984) Modeling of catalytic char gasification. Industrial Engineering Chemistry Fundamentals 23:223–229
37. Smedowski Ł, Krzesinska M, Kwasny W, Kozanecki M (2011) Development of ordered structures in the high-temperature (HT) cokes from binary and ternary coal blends studied by means of X-ray diffraction and Raman spectroscopy. Energy Fuels 25:3142–3149
38. Zhang Y, Kang X, Tan J, Frost RL (2013) Influence of Calcination and Acidification on Structural Characterization of Anyang Anthracites. Energy Fuels 27:7191–7197
39. Asadullah M, Zhang S, Min Z, Yimsiri P, Li CZ (2010) Effects of biomass char structure on its gasification reactivity. Bioresour Technol 101:7935–7943
40. Cuesta DP, Laureyns A (1994) J, et al., Raman microprobe studies on carbon materials[J]. Carbon 32(8):1523–1532
41. Jiang J, Yang W, Cheng Y, Liu Z, Zhang Q, Zhao K (2019) Molecular structure characterization of middle-high rank coal via XRD, Raman and FTIR spectroscopy: Implications for coalification. Fuel 239:559–572
42. Jawhari T, Roid A, Casado JJC, Raman spectroscopic characterization of some commercially available carbon black materials, 33 (1995) 1561–1565

43. Walker PL, Matsumoto S, Hanzawa T, Muira T, Ismail IMK, Walker PL, Matsumoto S, Hanzawa T, Muira T, Ismail IMK (1983) Catalysis of Gasification of Coal-derived Cokes and Chars. Fuel 62:140–149
44. Mafu LD, Neomagus HWJP, Everson RC, Strydom CA, Carrier M, Okolo GN, Bunt JR (2017) Chemical and structural characterization of char development during lignocellulosic biomass pyrolysis. Bioresour Technol 243:941–948

Figures

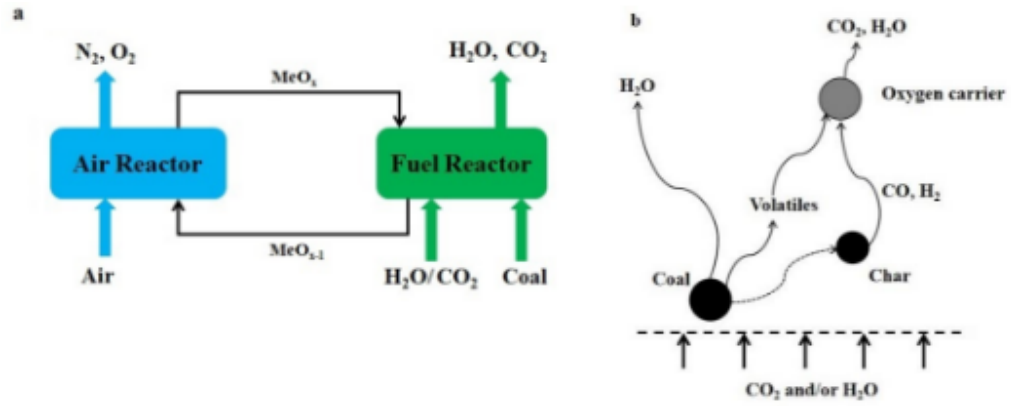

Figure 1

Simplified schematic iG-CLC process

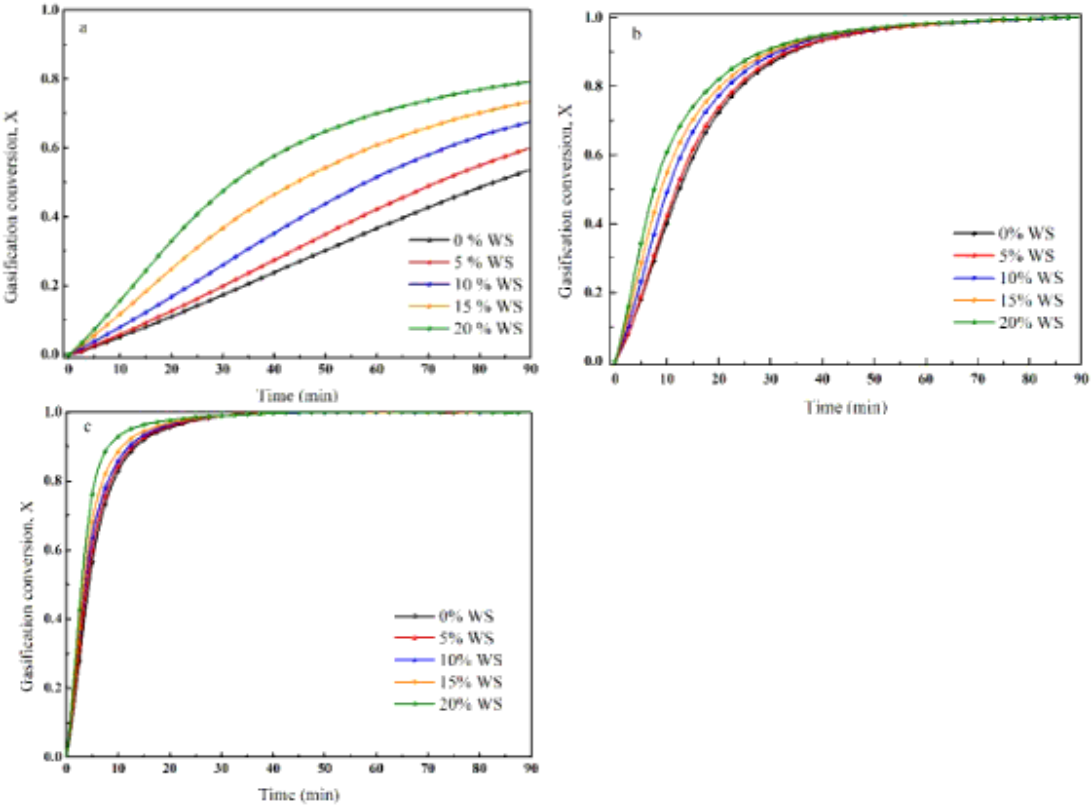

Figure 2

TGA profiles of gasification of co-pyrolysis chars of coal and biomass in CO2 at given temperatures (a: 950 °C, b: 1050 °C, c: 1150 °C).

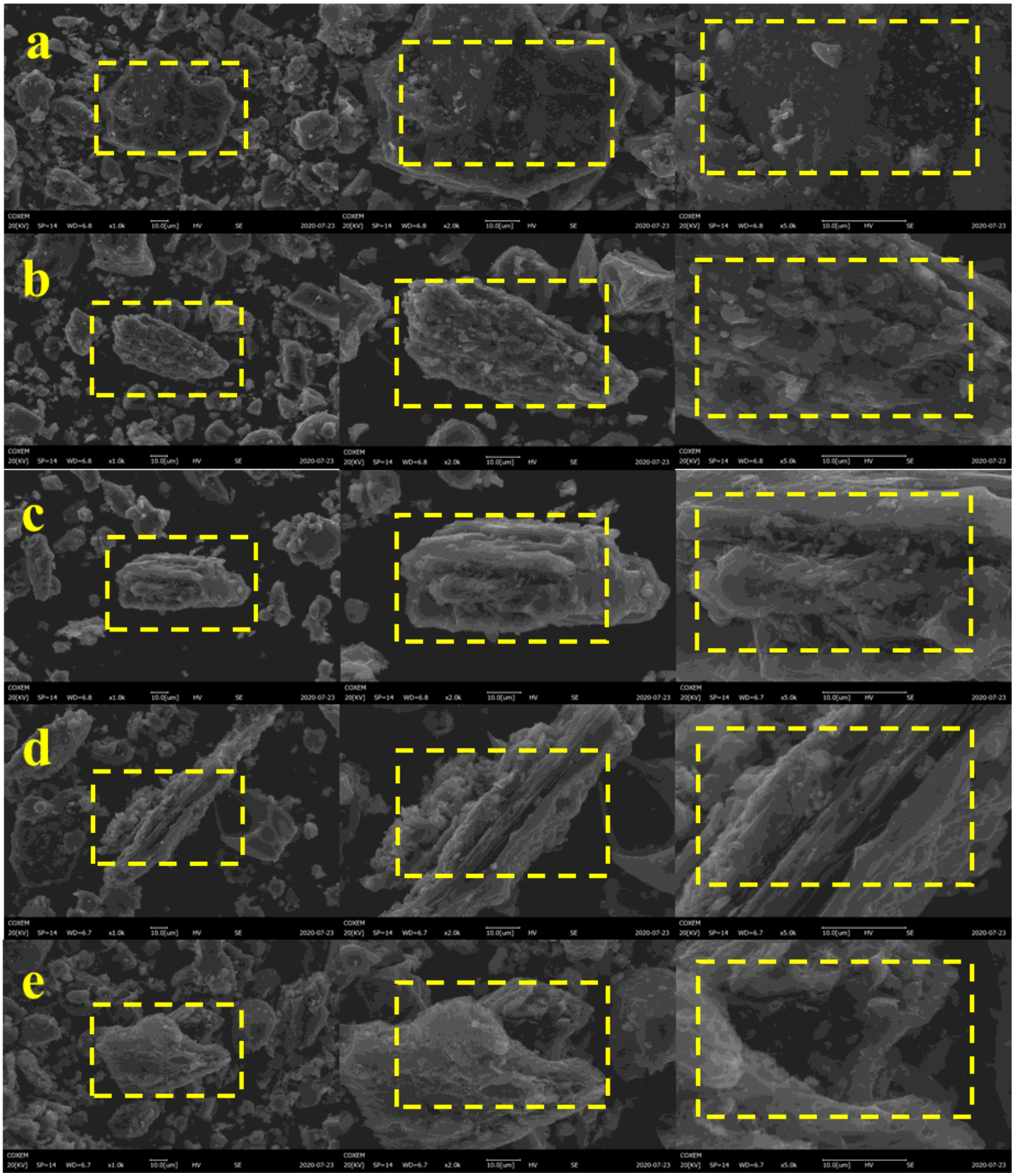

Figure 3

SEM micrographs co-pyrolysis char with different biomass ratio (a-e：0%-20%WS).

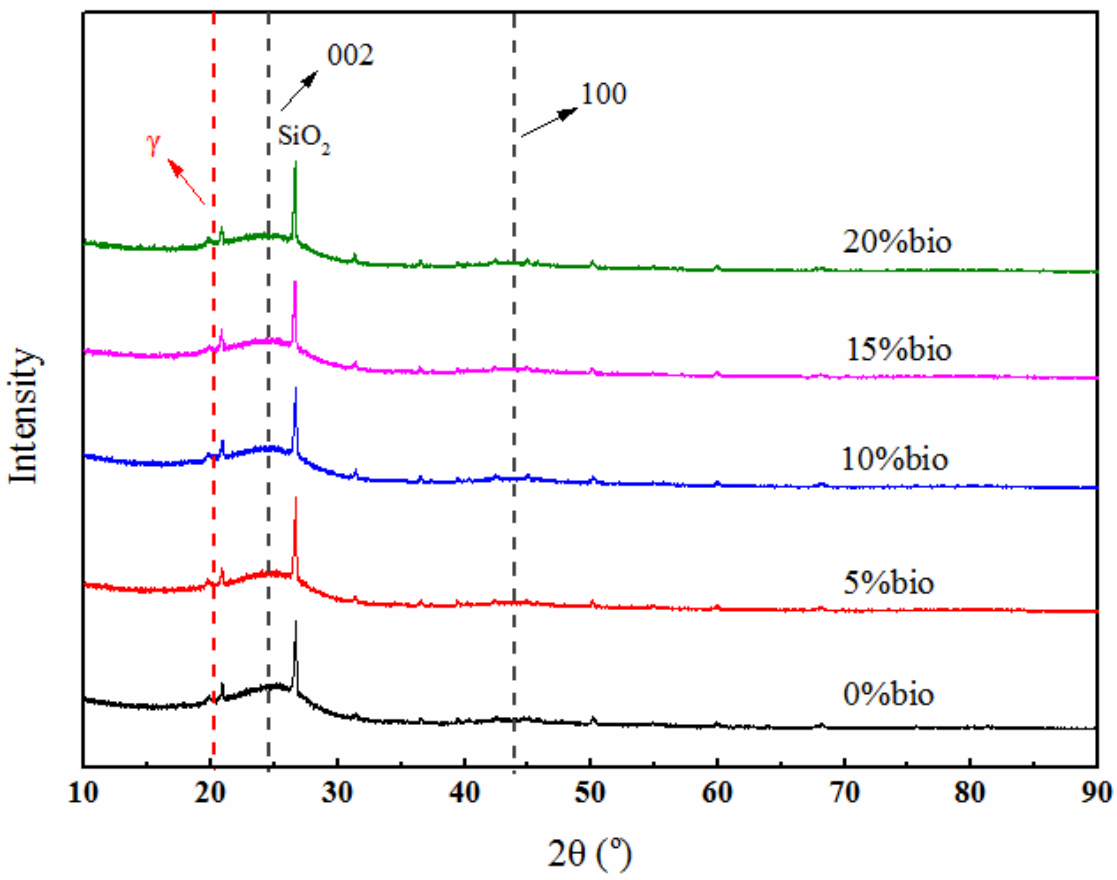

Figure 4

XRD spectra of the prepared char samples in the 2θ range of ~10–90°.

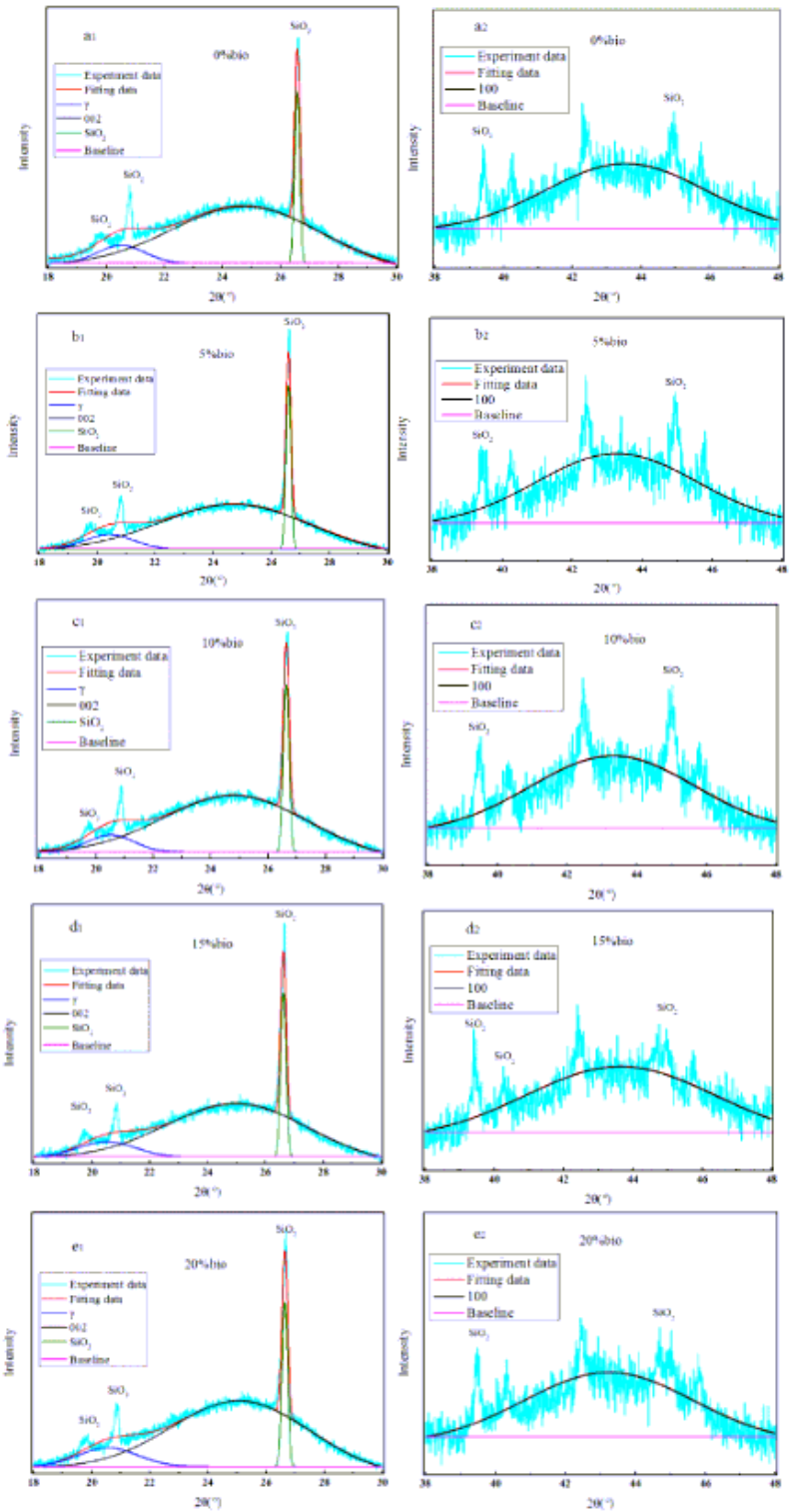

Figure 5

Curve-fitting of the XRD peaks for selected samples in the 2θ ranges of 18–30°

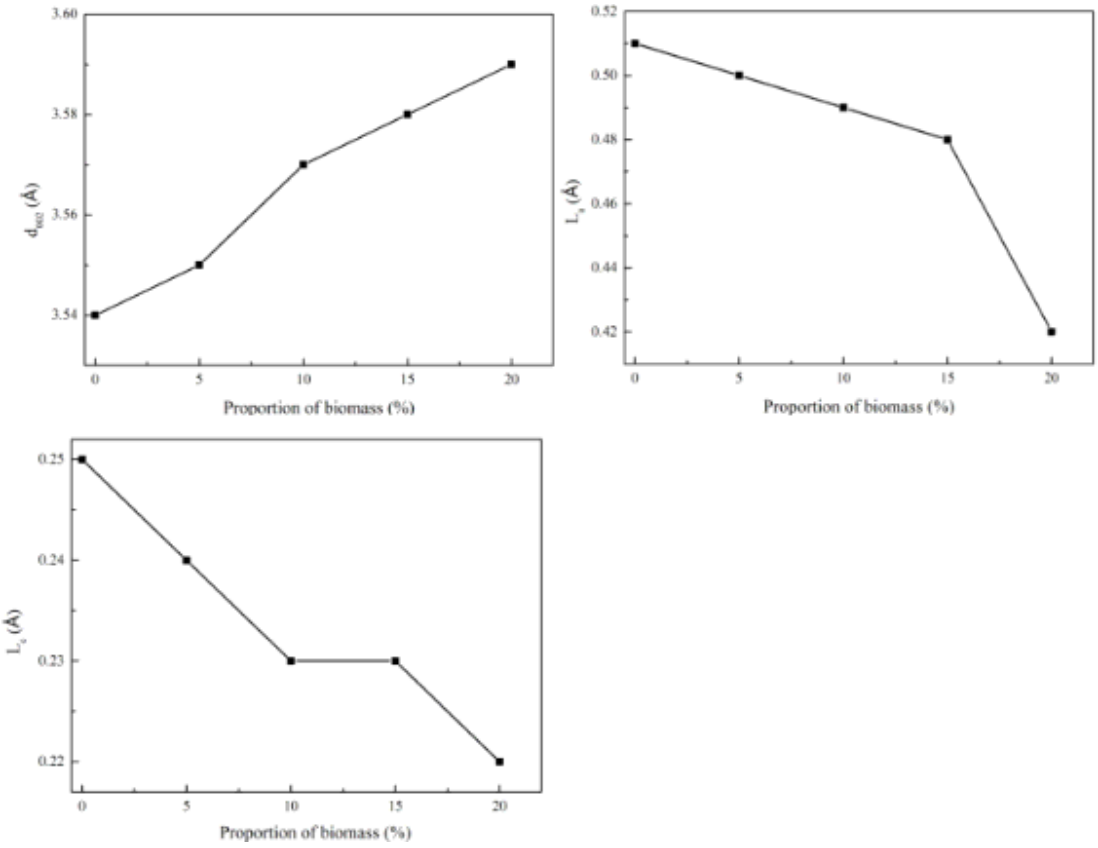

Figure 6

The relationship between the d002, La, and Lc values and the biomass proportion.

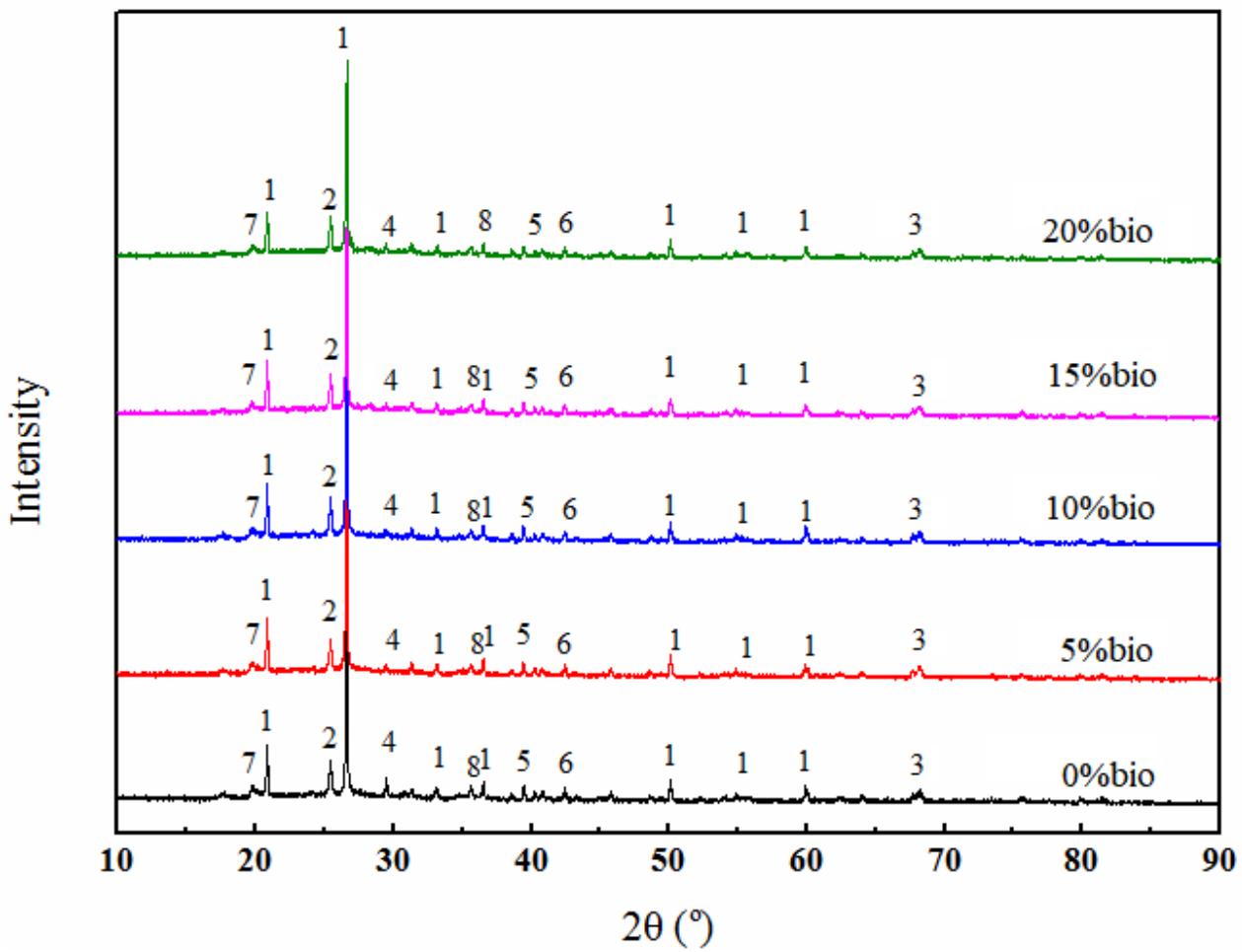

Figure 7

The XRD patterns of co-pyrolysis char ash (1-SiO2, 2-KAlSiO4, 3-Al2O3, 4-CaCO3, 5-Al2O3·2SiO2·2H2O□6-NaAlSi3O8, 7-Al2O3·2SiO2, 8-Fe2O3)

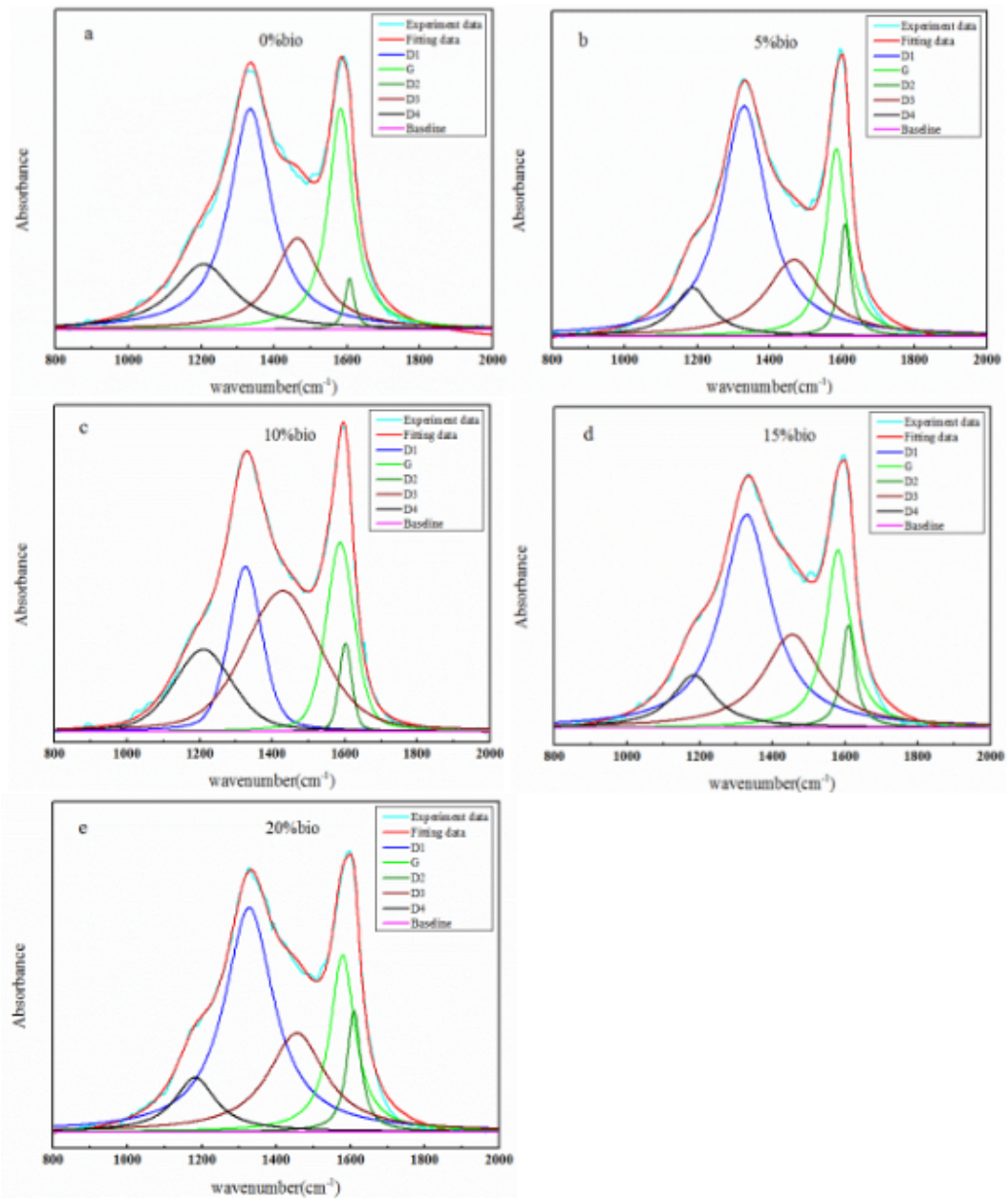

Figure 8

Raman spectra of selected chars.

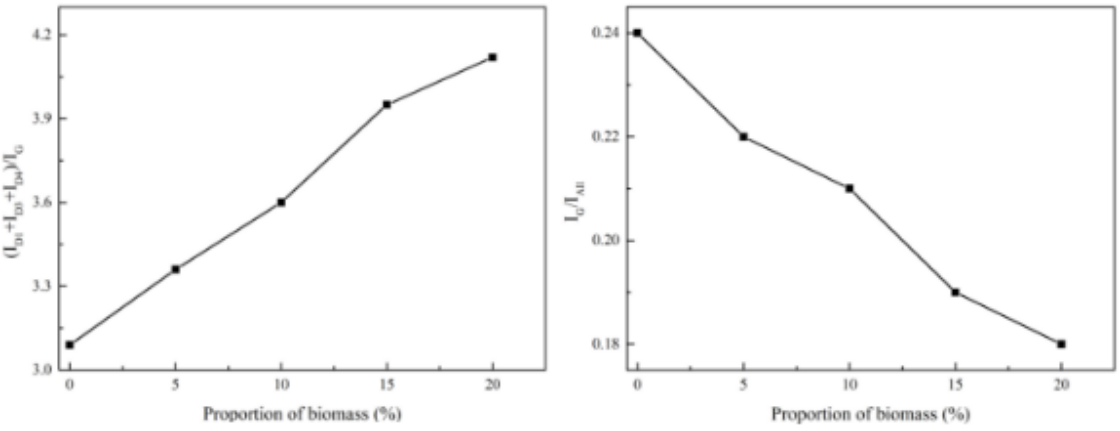

Figure 9

Variation of the band area ratios (ID1 + ID3 + ID4) / IG and IG / Iall with the changes in the biomass proportion.

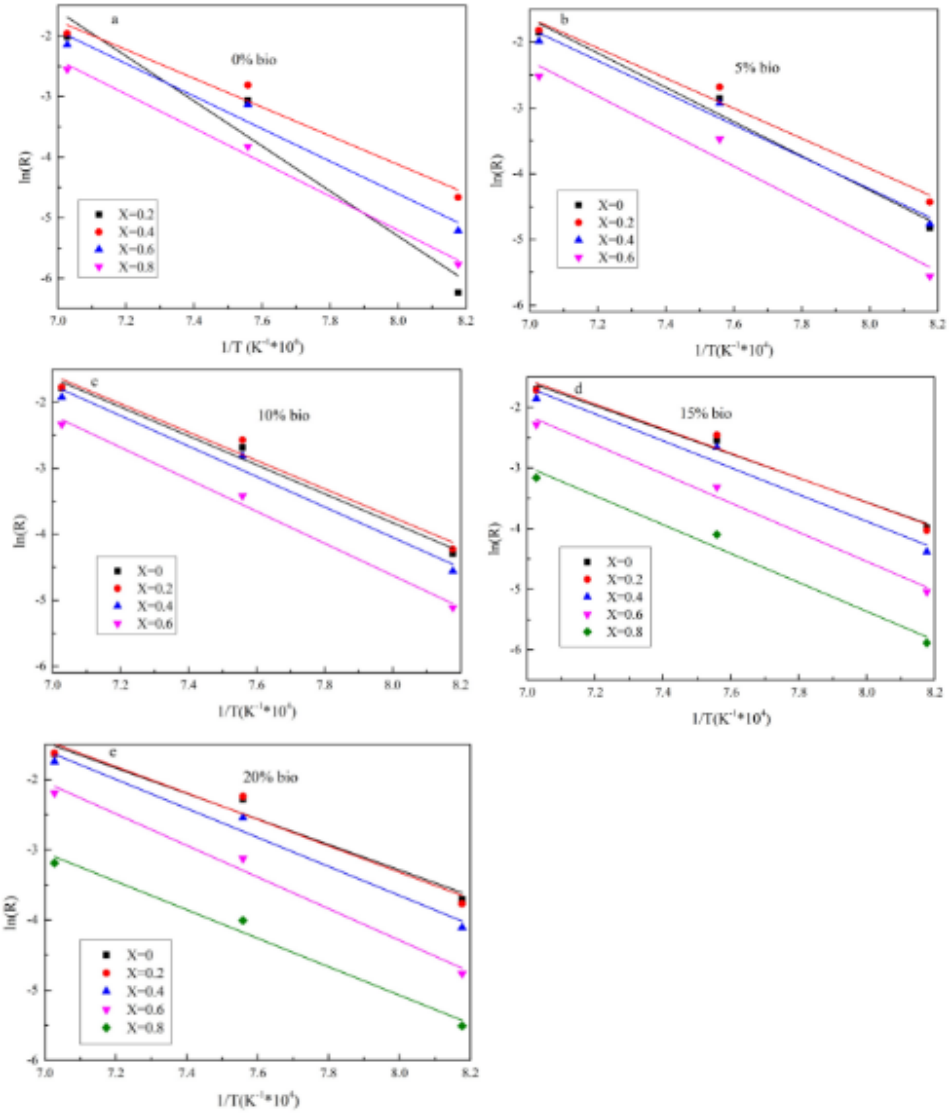

Figure 10

Relationship between ln(R) and 1/T

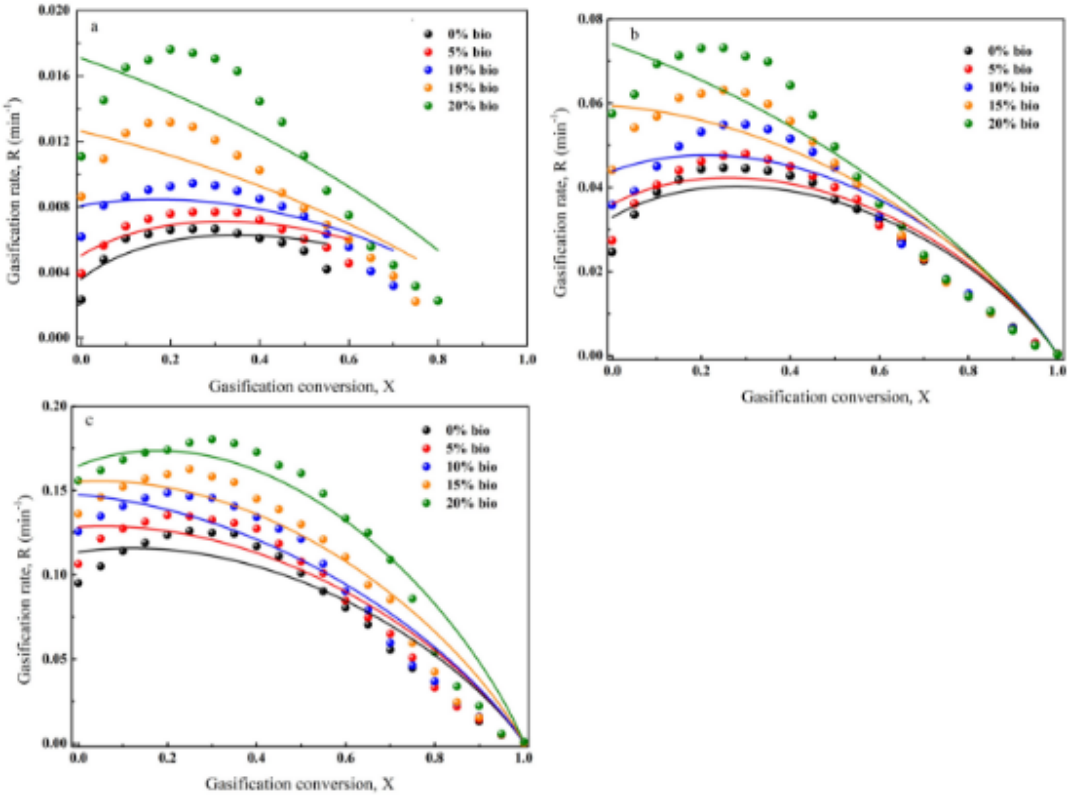

Figure 11

Application of RPM to define the gasification behaviour of chars at given temperatures (a: 950 °C, b: 1050 °C, c: 1150 °C).

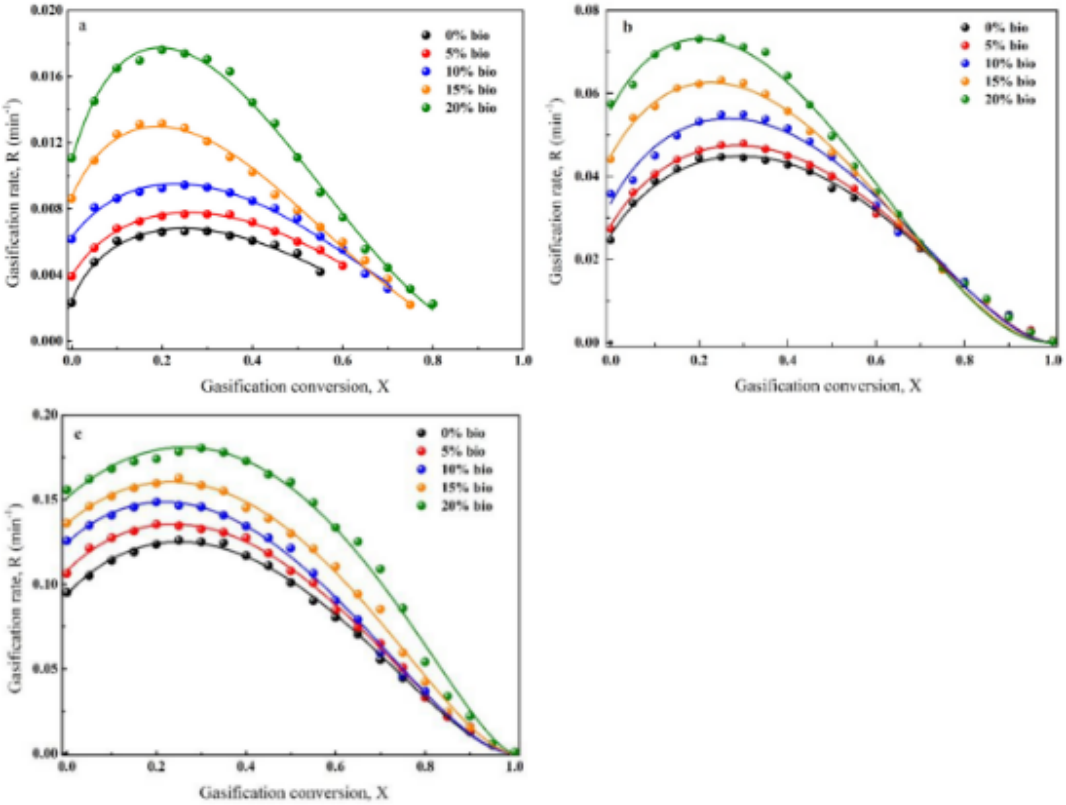

Figure 12

Application of eRPM to define the gasification behaviour of chars at given temperatures (a: 950 °C, b: 1050 °C, c: 1150 °C).

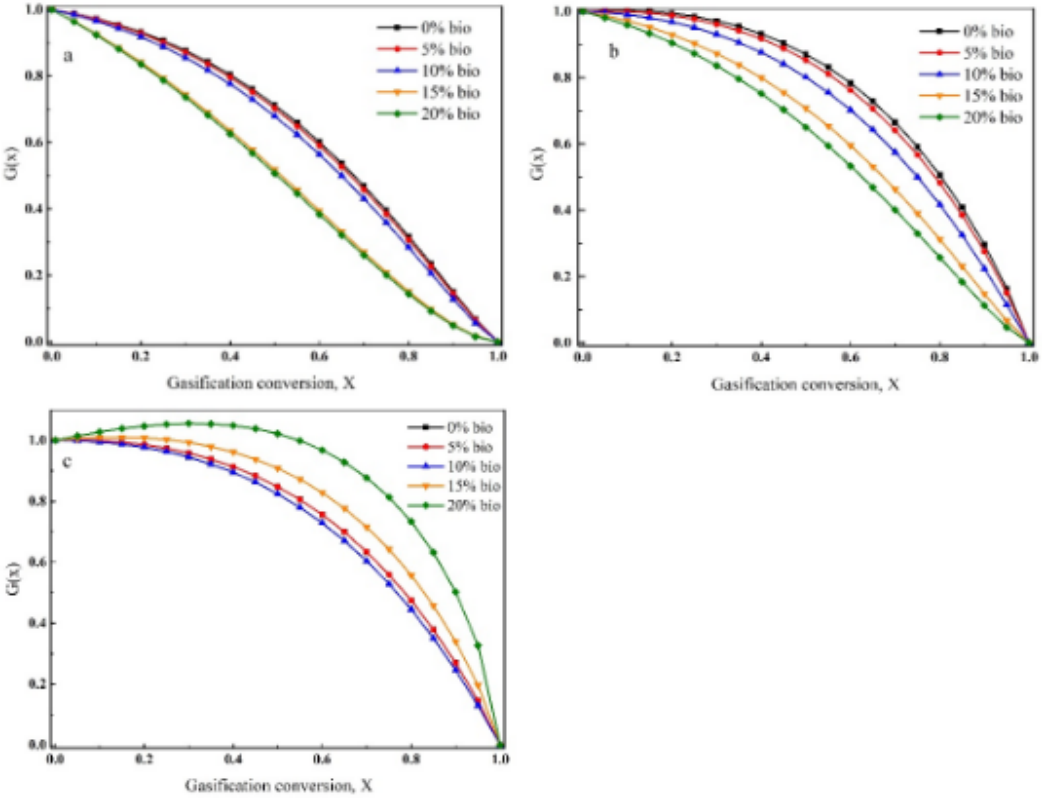

Figure 13

synergistic influence effects of the interactions between chars and minerals as well as between different minerals on the entire co-gasification process (a: 950 °C, b: 1050 °C, c: 1150 °C).

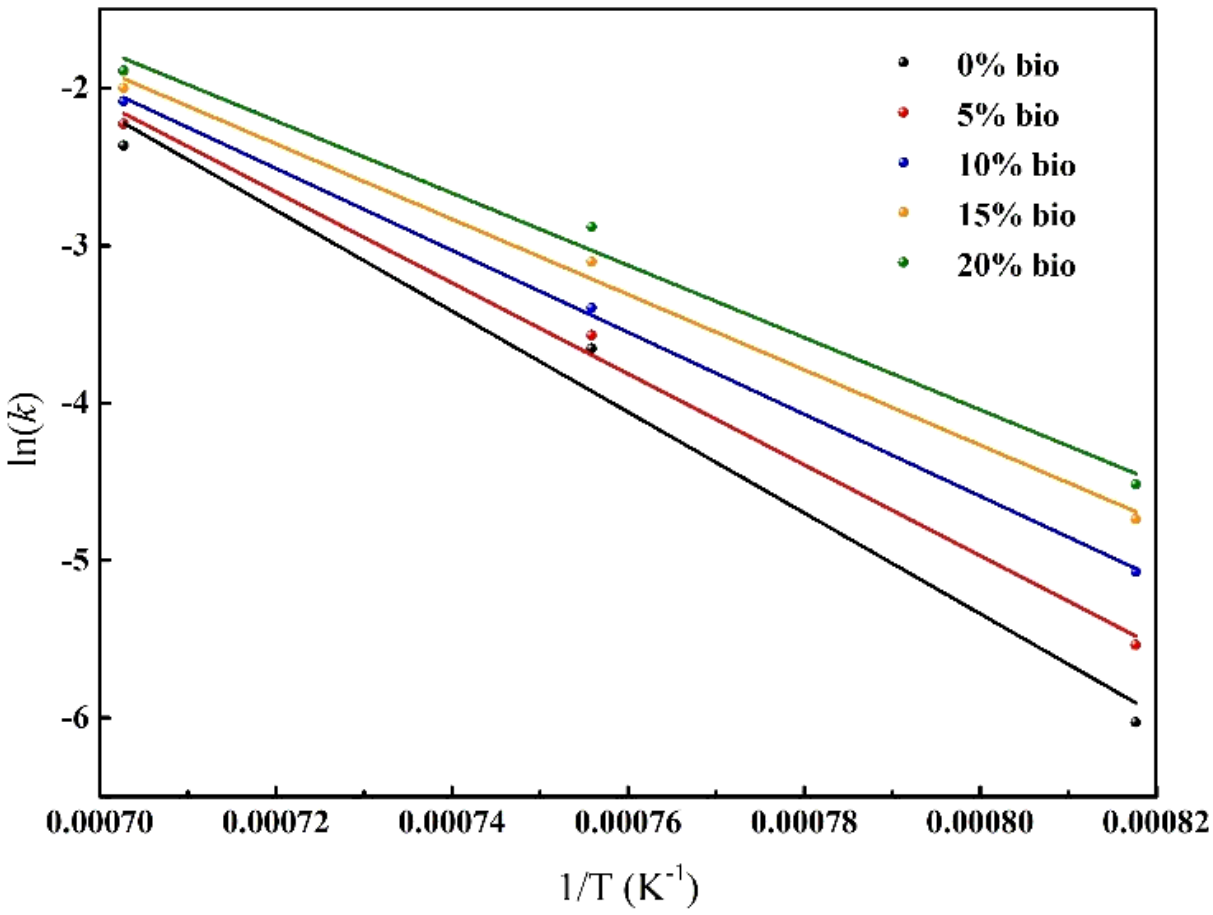

Figure 14

The correlation between lnk and 1/T for gasification of char samples.

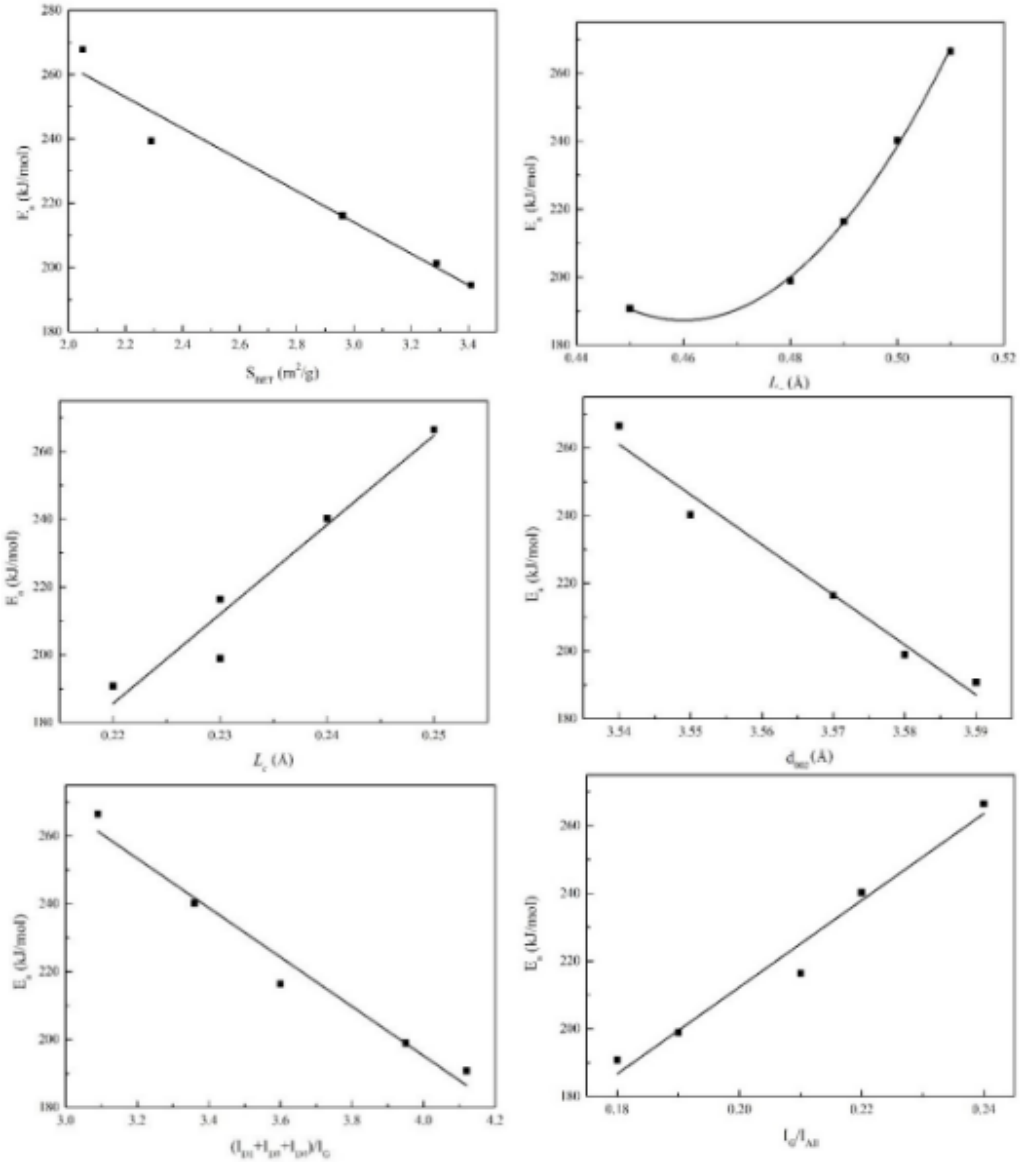

Figure 15

The relationship between the char characteristics and gasification reactivity.